

Data Release: Characterizing the transition from diffuse atomic to dense molecular clouds in the Magellanic clouds with [C II], [C I], and CO

Jorge L. Pineda¹, Paul F. Goldsmith¹, William D. Langer¹, Shinji Horiuchi², Thomas B. H. Kuiper¹, Erik Muller³, Annie Hughes⁴, Jürgen Ott⁵, Miguel A. Requena-Torres⁶, Thangasamy Velusamy¹, and Tony Wong⁷

¹*Jet Propulsion Laboratory, California Institute of Technology, 4800 Oak Grove Drive, Pasadena, CA 91109-8099, USA*

²*CSIRO Astronomy & Space Science/NASA Canberra Deep Space Communication Complex, PO Box 1035, Tuggeranong ACT 2901, Australia*

³*National Astronomical Observatory of Japan, Chile Observatory, Tokyo, Mita ka, 181-8588, Japan*

⁴*CNRS, IRAP, 9 Av. Colonel Roche, BP 44346, 31028, Toulouse Cedex 4, France ; Université de Toulouse, UPS-OMP, IRAP, 31028, Toulouse Cedex 4, France*

⁵*National Radio Astronomy Observatory, P.O. Box O, 1003 Lopezville Road, Socorro, NM 87801, USA*

⁶*Space Telescope Science Institute, 3700 San Martin Dr., Baltimore, 21218 MD, USA*

⁷*Department of Astronomy, University of Illinois, Urbana, IL 61801, USA*

Jorge.Pineda@jpl.nasa.gov

1. Introduction

In Pineda et al. (2017), we presented deep observations of the [C II] 158 μm , [C I] 609 μm , [C I] 370 μm , and ^{12}CO $J = 7 \rightarrow 6$ lines towards 54 LMC and SMC lines-of-sight (LOS) that represent different stages of cloud evolution. These data were obtained using the HIFI (de Graauw et al. 2010) instrument onboard the *Herschel Space Observatory*¹ (Pilbratt et al. 2010). We complemented this data set with observations of the $J = 1 \rightarrow 0$ and $J = 3 \rightarrow 2$ transitions of ^{12}CO and ^{13}CO from the ATNF Mopra² and APEX³ telescopes, respectively. We base our target selection on maps of H I, 160 μm dust continuum emission, and CO emission as well as on results from the FUSE survey of H₂ absorption towards the Magellanic Clouds (Cartledge et al. 2005). The targets are distributed throughout the LMC and SMC in order to study spatial variations of the properties of their ISM. By studying clouds at different stages of evolution our goal was to determine the key factors that characterize the evolution of the interstellar matter in the Magellanic clouds. We refer to Pineda et al. 2017 for details on the data reduction and survey strategy. We show the locations used in our analysis in Figure 1.

In this document we describe our release of the [C II] 158 μm , [C I] 609 μm , [C I] 370 μm , and ^{12}CO $J = 7 \rightarrow 6$ lines observed with *Herschel*/HIFI. In Figure 2 to 17, we present the spectra of all observed lines for our sample. The plots include supplementary ^{12}CO and ^{13}CO $J = 1 \rightarrow 0$ observations done with the ATNF Mopra telescope (project M580), ^{12}CO and ^{13}CO $J = 3 \rightarrow 2$ observations done with the APEX

¹*Herschel* is an ESA space observatory with science instruments provided by European-led Principal Investigator consortia and with important participation from NASA.

²The Mopra radio telescope is part of the Australia Telescope which is funded by the Commonwealth of Australia for operation as a National Facility managed by CSIRO.

³This publication is based in part on data acquired with the Atacama Pathfinder Experiment (APEX). APEX is a collaboration between the Max-Planck-Institut für Radioastronomie, the European Southern Observatory, and the Onsala Space Observatory

telescope, and H I 21 cm spectra taken from maps of the entire LMC and SMC presented by Kim et al. (2003) and Stanimirovic et al. (1999) (see also Staveley-Smith et al. 2003), respectively. This ancillary data set is available upon request.

2. Data Product Format

The final reduced spectra for this data release are in the form of ASCII files. The reduced data for each line of sight has a unique identification label, LOS-ID, in the following format: `LOS_LINE_tmb.dat`, where the first term (`LOS`) gives the name of the observed line-of-sight, and the second term (`LINE`) corresponds to the spectral line observed. Each data file also contains a header with information about the observations, including the observing mode, the Right Ascension (J2000), Declination (J2000), the Herschel observation identification numbers, OBSIDs, and two columns, the first gives the LSR Velocity in km/s and the second is the spectral line Main Beam Temperature, T_{mb} , in Kelvins. The Header has the following information and format:

```
# PROPOSAL OT1_jpineda_1
# INSTRUMENT xxxx
# SOURCE wwww
# LINE zzz
# RA xxx
# DEC yy
# OBSID xxxxxxxx , yyyy/yyyy
# COLUMN1 LSR VELOCITY [km/s]
# COLUMN2 MAIN BEAM TEMPERATURE [K]
```

A sample data file is given below showing the header and a partial list of data values for a [C II] spectrum in the PDR1_NW LOSs

```
# PROPOSAL OT1_jpineda_1
# INSTRUMENT HERSCHEL/HIFI
# SOURCE PDR1_NW
# LINE [CII]
# RA 5:25:46.90
# DEC -66:13:41.6
# OBSID 1342232662
# COLUMN1 LSR_VELOCITY [km/sec]
# COLUMN2 MAIN BEAM TEMPERATURE [K]
-3.9514207839966 -0.210869
-3.1627161502838 0.0878029
-2.3740117549896 -0.272805
-1.5853071212769 -0.157038
-0.79660266637802 0.0628355
-7.8981323167682E-03 -0.170687
0.78080636262894 -0.121548
...
```

...
...
...
392.76696777344 0.0898715
393.5556640625 0.0941881
394.34436035156 -0.0327054
395.13305664063 0.101491
395.92178344727 0.104604
396.71047973633 0.0967738
397.49917602539 0.110687
398.28787231445 0.0391588
399.07659912109 -0.040982
399.86529072117 0.0385313

In Table 1 (below) and in the archive Lookup Table, we list all observed positions with the LOS-ID, exact coordinates used for the pointing, and the OBSIDs. We refer the user interested in reconstructing the spectra, or wanting additional details about the observations, including the reference positions, to the Herschel OBSIDs.

3. Acknowledgments

We thank the staffs of the ESA and the NASA Herschel Science Centers for their invaluable help with the data reduction routines. This work was performed at the Jet Propulsion Laboratory, California Institute of Technology, under contract with the National Aeronautics and Space Administration. ©2016 California Institute of Technology. Government sponsorship acknowledged.

REFERENCES

- Cartledge, S. I. B., Clayton, G. C., Gordon, K. D., et al. 2005, ApJ, 630, 355
de Graauw, T., Helmich, F. P., Phillips, T. G., et al. 2010, A&A, 518, L6+
Kim, S., Staveley-Smith, L., Dopita, M. A., et al. 2003, ApJS, 148, 473
Meixner, M., Panuzzo, P., Roman-Duval, J., et al. 2013, AJ, 146, 62
Pilbratt, G. L., Riedinger, J. R., Passvogel, T., et al. 2010, A&A, 518, L1+
Pineda, J. L., Langer, W. D., Goldsmith, P. F., et al. 2017, ApJ, 839, 107
Stanimirovic, S., Staveley-Smith, L., Dickey, J. M., Sault, R. J., & Snowden, S. L. 1999, MNRAS, 302, 417
Staveley-Smith, L., Kim, S., Calabretta, M. R., Haynes, R. F., & Kesteven, M. J. 2003, MNRAS, 339, 87
Wong, T., Hughes, A., Ott, J., et al. 2011, ApJS, 197, 16

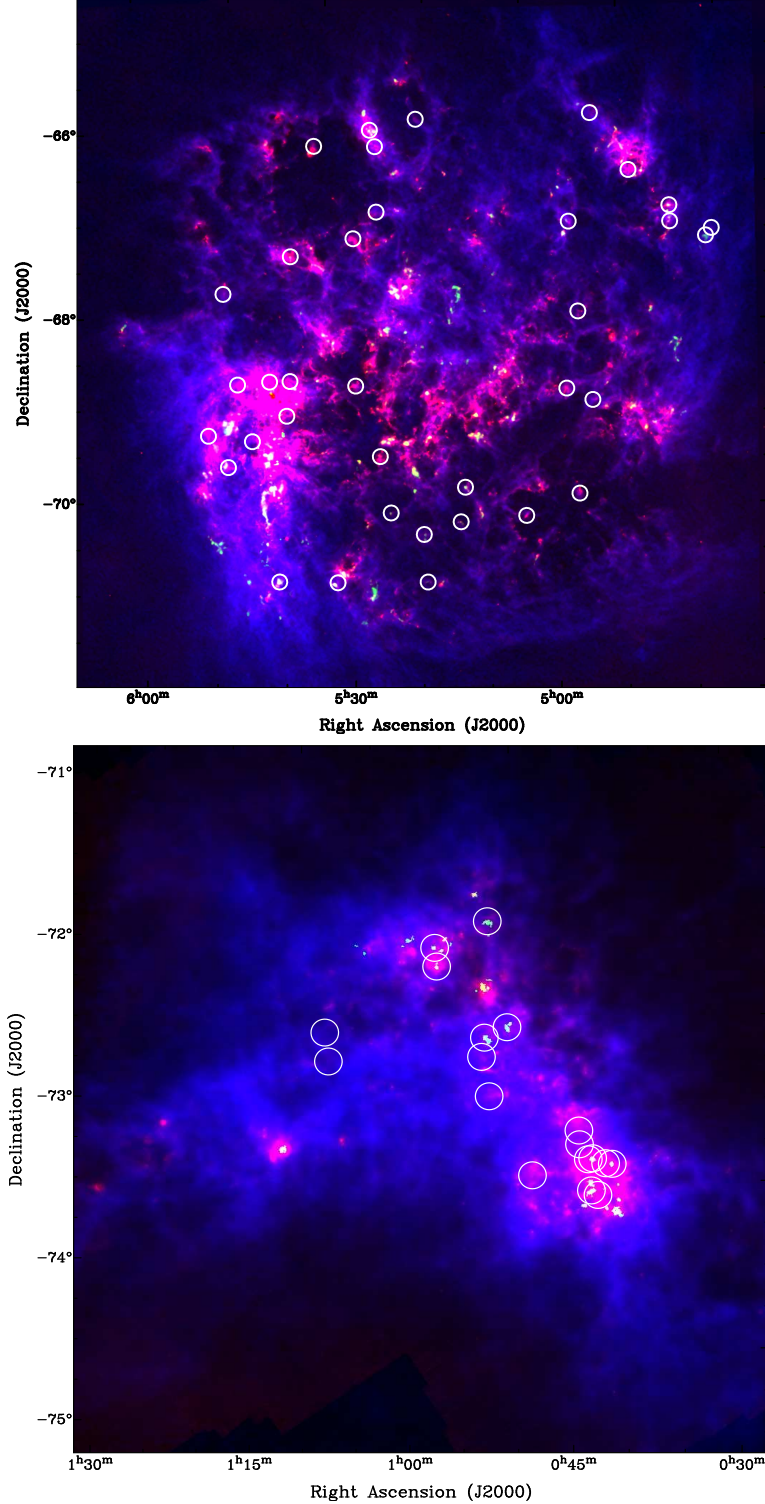


Fig. 1.— Images showing H^0 column density map (blue; Kim et al. 2003, Stanimirovic et al. 1999), *Herschel* 160 μm continuum emission (red; Meixner et al. 2013), and MAGMA CO line emission (green; Wong et al. 2011 and Muller et al. 2016 in preparation) in the Large (*top*) and Small (*bottom*) Magellanic clouds. The white circles denote the positions of the spectra in the database. The size of the circles does not denote the beam size employed in any of the observations presented here.

Table 1. Summary of Observed Lines of Sight and Corresponding OBSIDs

LOS	R.A. (J2000)	Decl. (J2000)	[C II]	[C I] ${}^3\text{P}_1 - {}^3\text{P}_0$	[C I] ${}^3\text{P}_2 - {}^3\text{P}_1$ & ${}^{12}\text{CO}(7 - 6)$ OBSID
Large Magellanic Cloud					
Diff1_NW	5:31:59.160	-66:22:52.30	1342232663	1342244792	1342245303
Diff2_SE	4:59:35.530	-70:11:04.60	1342235795	1342235819	1342245292
Diff3_Ridge	5:31:50.570	-71:12:41.60	1342244587	1342245603	1342245294
Diff4_NE	5:01:47.740	-65:59:05.20	1342232675	1342237610	1342245288
Diff5_SE	4:58:53.950	-69:08:29.90	1342232668	1342245606	1342245291
Diff6_NW	5:43:34.910	-67:56:08.20	1342232667	1342245602	1342245298
Diff7_NW	5:25:17.310	-67:08:03.60	1342232664	1342245601	1342245299
LMC10_NE	4:51:51.130	-67:05:45.00	1342232673	1342244796	1342234309
LMC11_Ridge	5:25:33.790	-69:50:16.60	1342238184	1342244798	1342245296
LMC12_SE	5:02:13.730	-69:02:16.40	1342238664	1342244797	1342245290
LMC_1_NW	5:28:01.860	-67:25:14.00	1342232666	1342244793	1342238214
LMC2_NW	5:25:16.260	-66:24:40.80	1342232661	1342237611	1342245301
LMC3_NW	5:20:44.750	-66:06:58.20	1342232660	1342244794	1342245300
LMC4_Ridge	5:28:22.540	-69:02:58.10	1342235797	1342235822	1342238212
LMC5_SE	5:06:23.080	-70:28:08.70	1342235796	1342235820	1342245293
LMC7_RIDGE	5:45:06.940	-69:50:42.60	1342238663	1342218529	1342245295
LMC8_RIDGE	5:47:11.770	-69:28:35.10	1342235799	1342235824	1342234310
LMC9_NE	5:03:20.840	-67:11:44.20	1342232669	1342244795	1342245289
NT127	5:24:19.750	-70:27:48.70	1342238188	1342227405	1342239578
NT2_NE	4:47:36.800	-67:12:13.70	1342232656	1342245607	1342238216
NT74	5:14:33.360	-70:10:51.90	1342239292	1342235821	1342239582
NT77	5:15:03.060	-70:33:49.60	1342244586	1342245605	1342239581
NT97	5:19:27.780	-71:13:52.40	1342244585	1342237612	1342239579
NT99	5:19:57.600	-70:42:21.70	1342239291	1342245604	1342239580
PDR1_NW	5:25:46.900	-66:13:41.60	1342232662	1342245600	1342245302
PDR2_NW	5:35:22.400	-67:35:00.50	1342232665	1342234312	1342238213
PDR3_NE	4:52:08.270	-66:55:13.70	1342232671	1342245609	1342238218
PDR4_RIDGE	5:39:48.670	-71:09:27.40	1342244588	1342235823	1342238211
SK-66D35	4:57:04.500	-66:34:38.00	1342232674	1342245610	1342245287
SK-67D2	4:47:04.400	-67:06:53.00	1342232672	1342245608	1342238217
SK-68D129	5:36:26.800	-68:57:32.00	1342238185	1342227171	–
SK-68D140	5:38:57.300	-68:56:53.00	1342238187	1342227170	1342245297
SK-68D155	5:42:54.900	-68:56:54.00	1342235798	1342227169	1342235097
SK-68D26	5:01:32.200	-68:10:43.00	1342232670	1342227172	1342238215

Table 1—Continued

LOS	R.A. (J2000)	Decl. (J2000)	[C II]	[CI] ${}^3\text{P}_1 - {}^3\text{P}_0$	[CI] ${}^3\text{P}_2 - {}^3\text{P}_1$ & ${}^{12}\text{CO}(7 - 6)$
				OBSID	
SK-69D228	5:37:09.200	-69:20:20.00	1342238186	1342227168	—
SK-69D279	5:41:44.700	-69:35:15.00	1342238189	1342227167	—
Small Magellanic Cloud					
AzV18	0:47:13.100	-73:06:25.00	1342233283	1342232965	1342232989
AzV456	1:10:55.800	-72:42:55.00	1342235794	1342235818	1342235098
AzV462	1:11:25.900	-72:32:21.00	1342235793	1342235817	1342234308
SMC_B2_6	0:47:57.220	-73:17:16.40	1342233285	1342232966	1342232990 1342235103
SMC_HI_1	0:58:40.480	-72:34:52.40	1342233293	1342232974	1342232988
SMC_HI_2	0:57:35.700	-72:48:56.30	1342233292	1342232975	1342232987
SMC_HI_3	0:53:01.970	-73:15:27.90	1342233289	1342232968	1342232992
SMC_HI_4	0:48:41.510	-73:06:08.30	1342233288	1342232969	1342232993
SMC_HI_5	0:47:20.350	-73:18:28.40	1342233284	1342232970	1342232994
SMC_HI_6	0:49:53.240	-72:56:15.60	1342233291	1342232971	1342232995
SMC_HI_7	0:49:38.080	-73:01:14.20	1342233290	1342232972	1342232996
SMC_LIRS36	0:46:40.280	-73:06:10.50	1342233286	1342232973	1342232997 1342235102
SMC_LIRS49	0:48:21.110	-73:05:29.00	1342233287	1342232967	1342232991 1342235101
SMC_NE_1a	0:59:43.820	-71:44:47.00	1342235022	1342235814	1342235099
SMC_NE_3c	1:03:31.860	-71:57:01.10	1342235021	1342235815	1342234307
SMC_NE_3g	1:03:09.890	-72:03:46.90	1342235023	1342235816	1342235100
SMC_NE_4a_hi	0:56:58.420	-72:22:37.40	1342233295	1342232976	1342232985
SMC_NE_4c_low	0:58:36.730	-72:27:44.20	1342233294	1342232977	1342232986

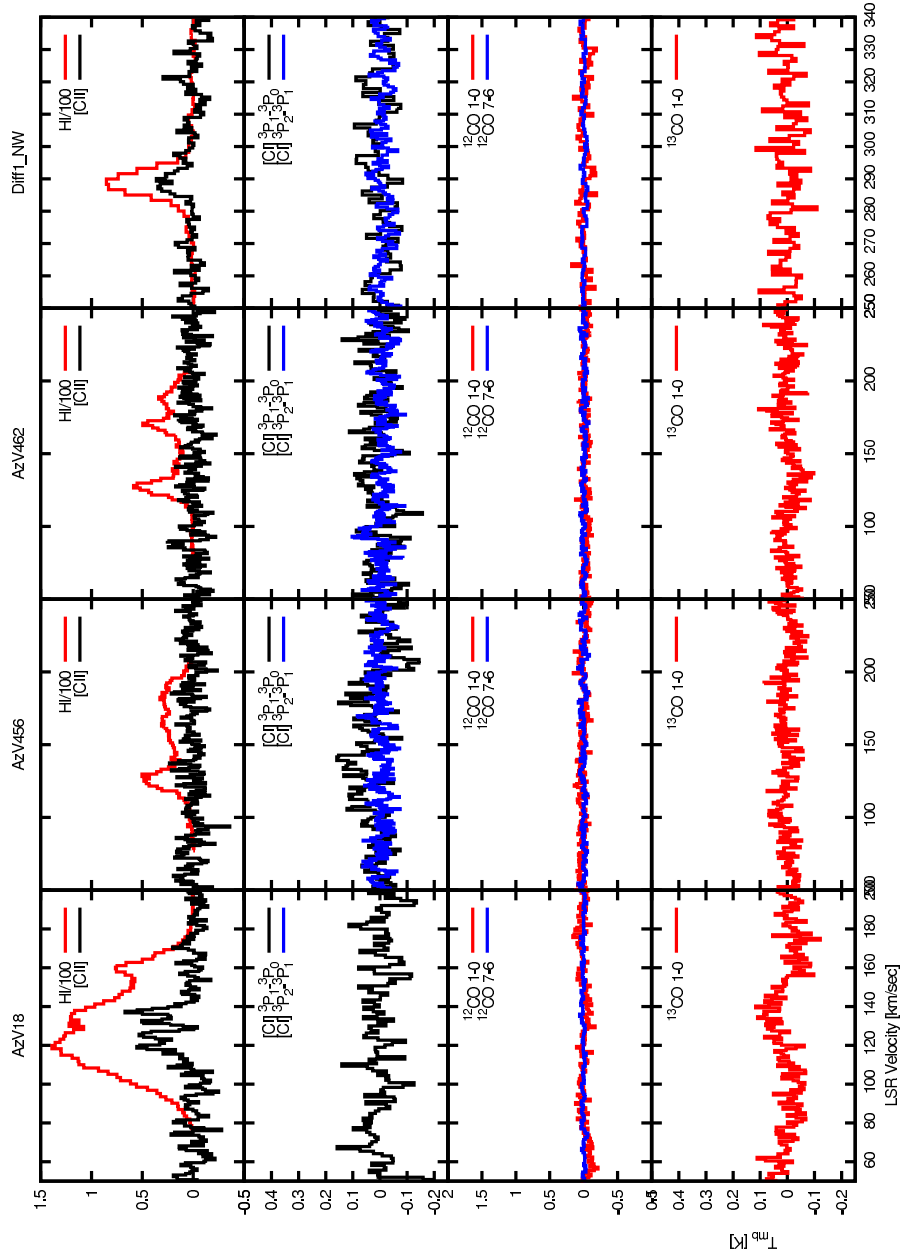


Fig. 2.— Spectra of every transition observed in the Large and Small Magellanic Clouds and stored in the database.

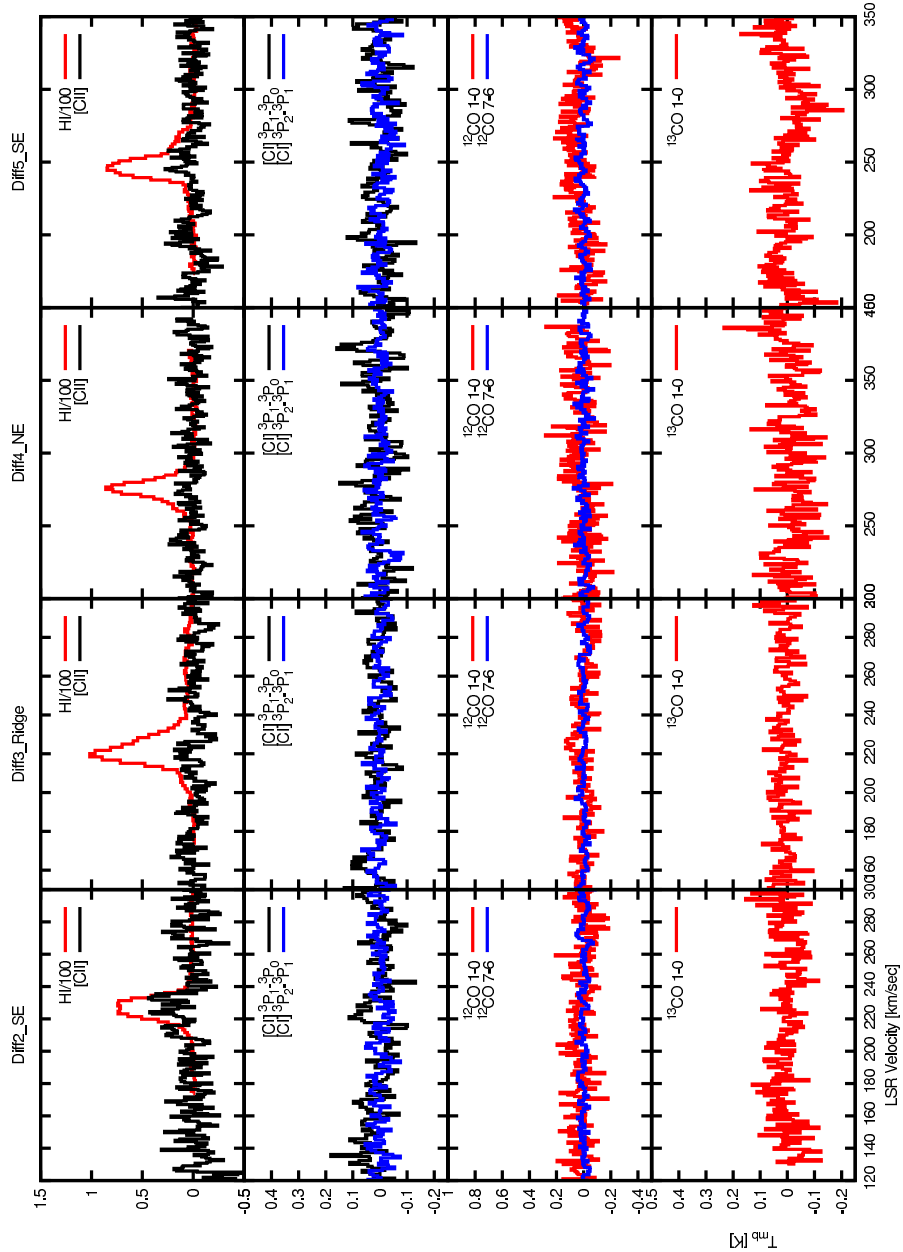


Fig. 3.— (Continued.)

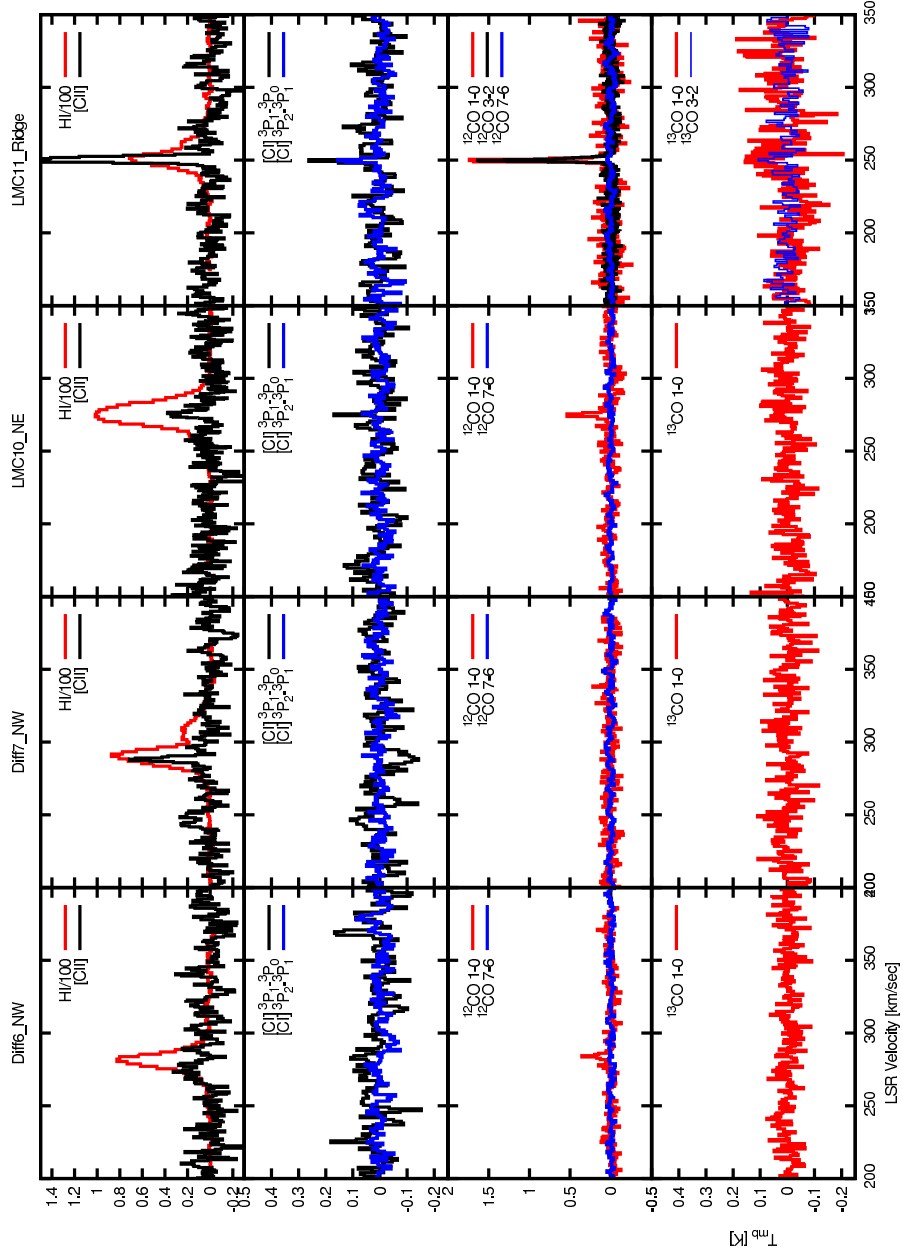


Fig. 4.— (Continued.)

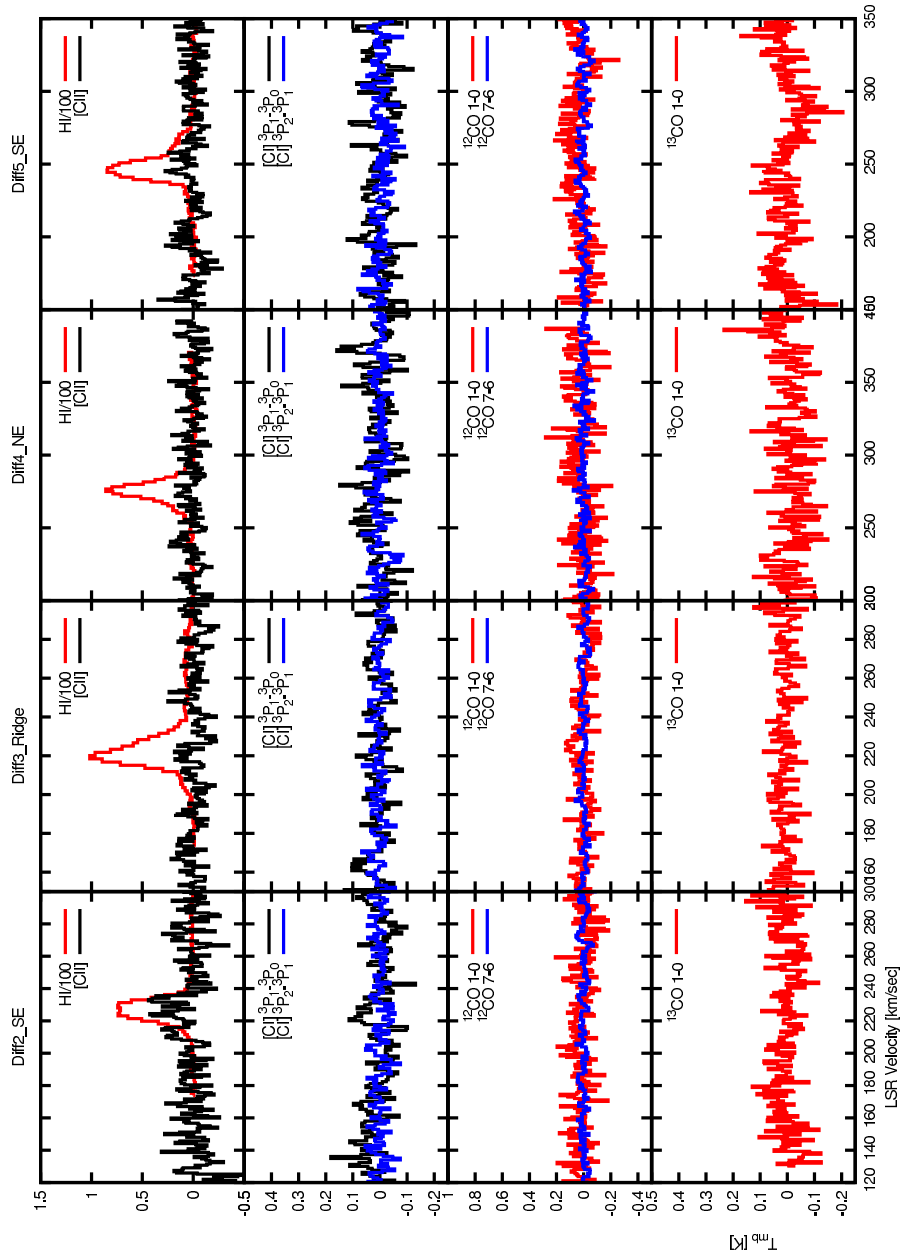


Fig. 5.— (Continued.)

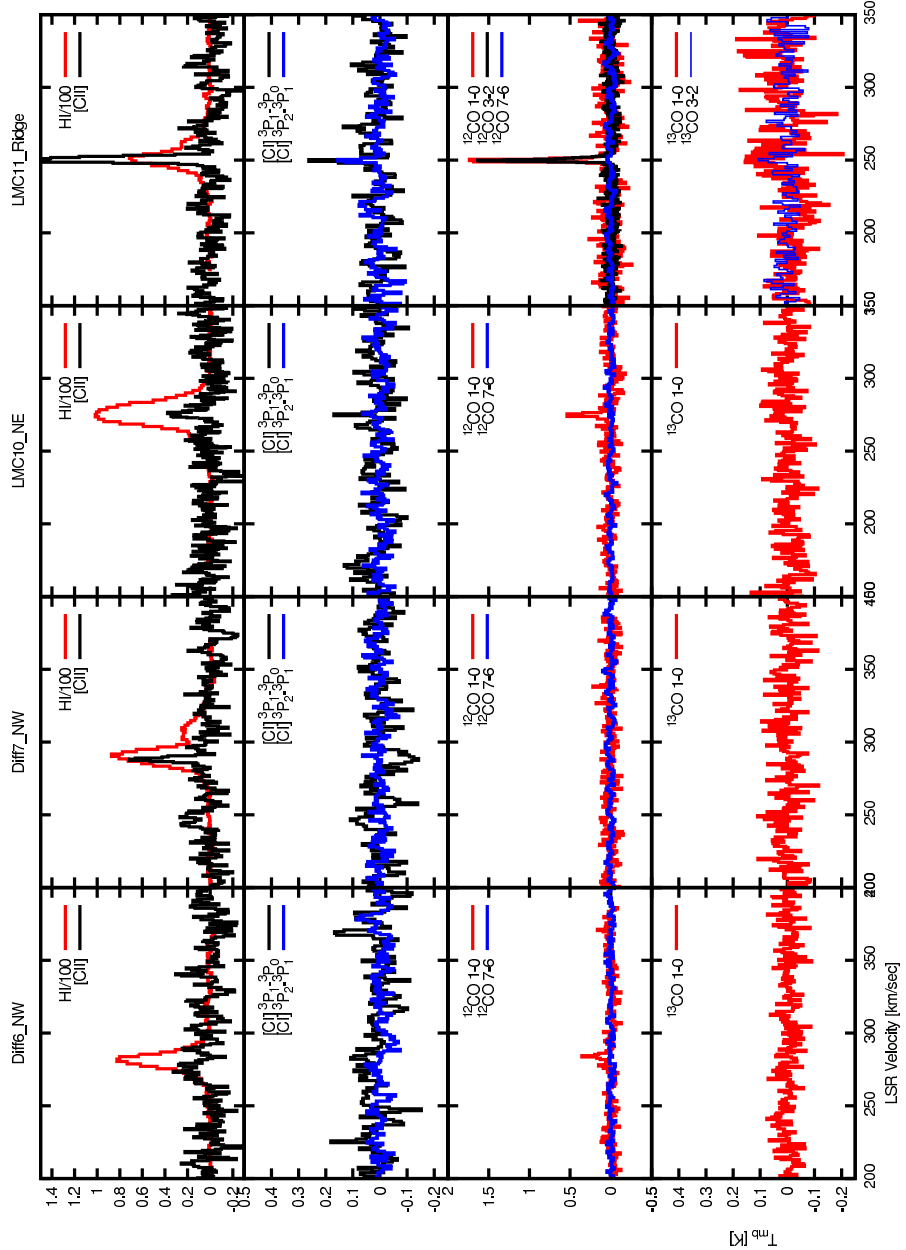


Fig. 6.— (Continued.)

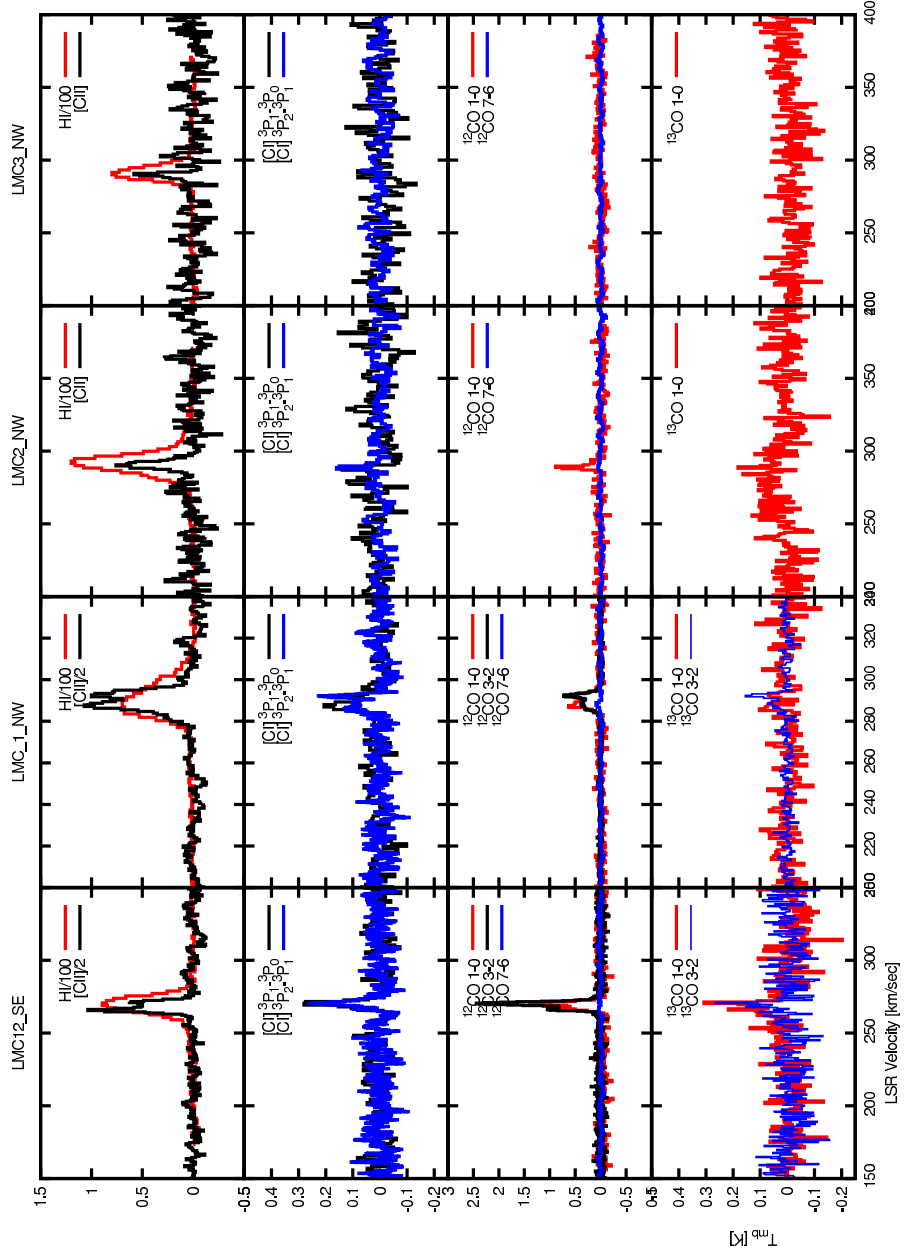


Fig. 7.— (Continued.)

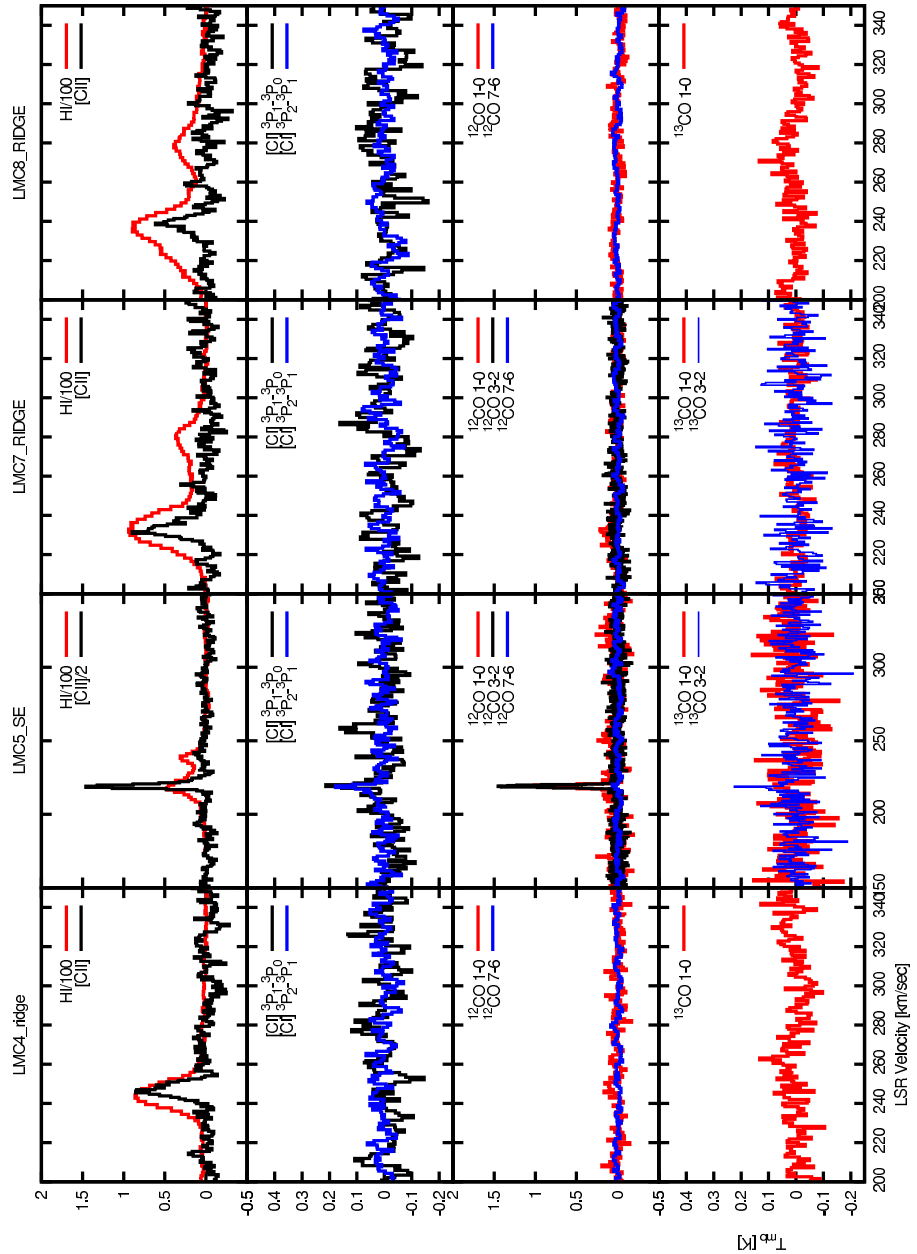


Fig. 8.— (Continued.)

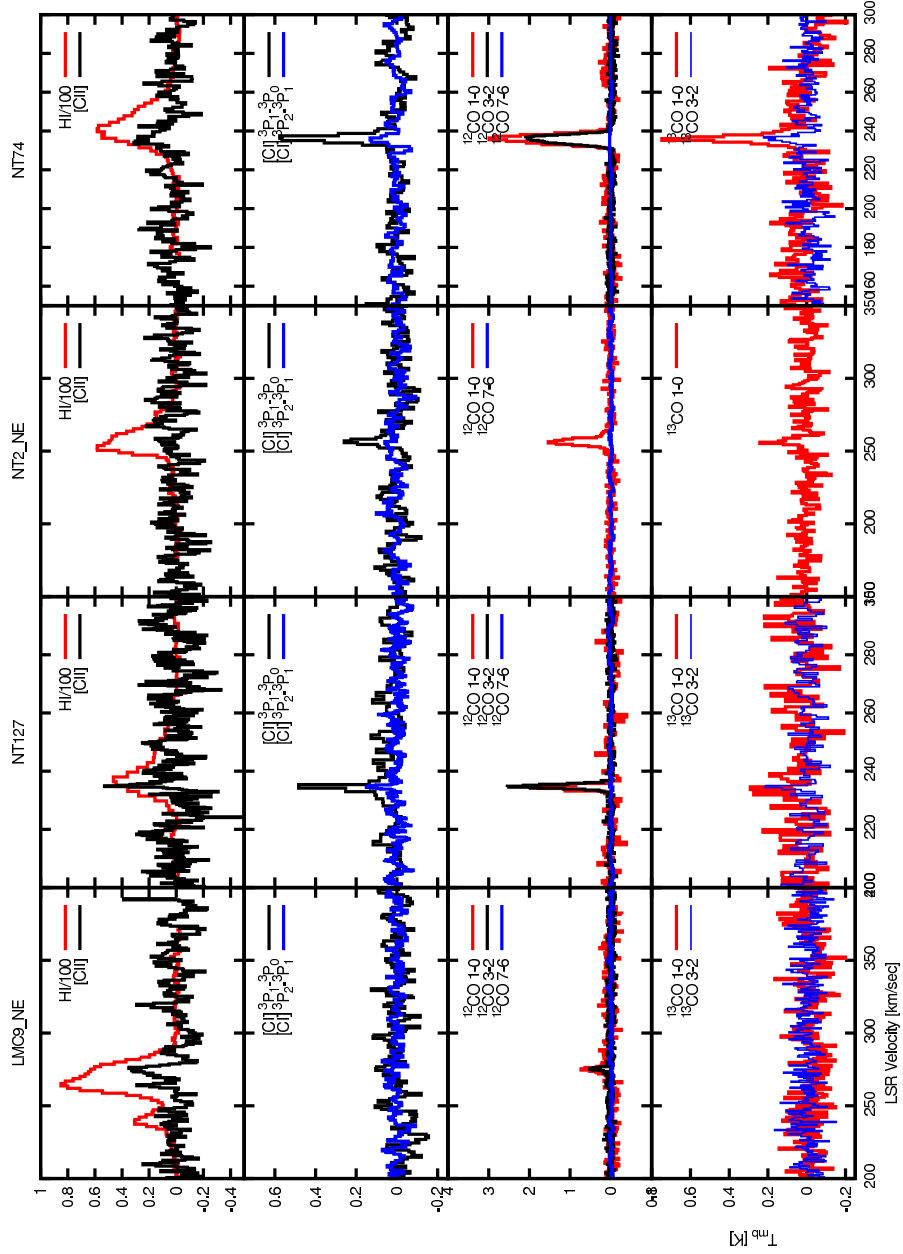


Fig. 9.— (Continued.)

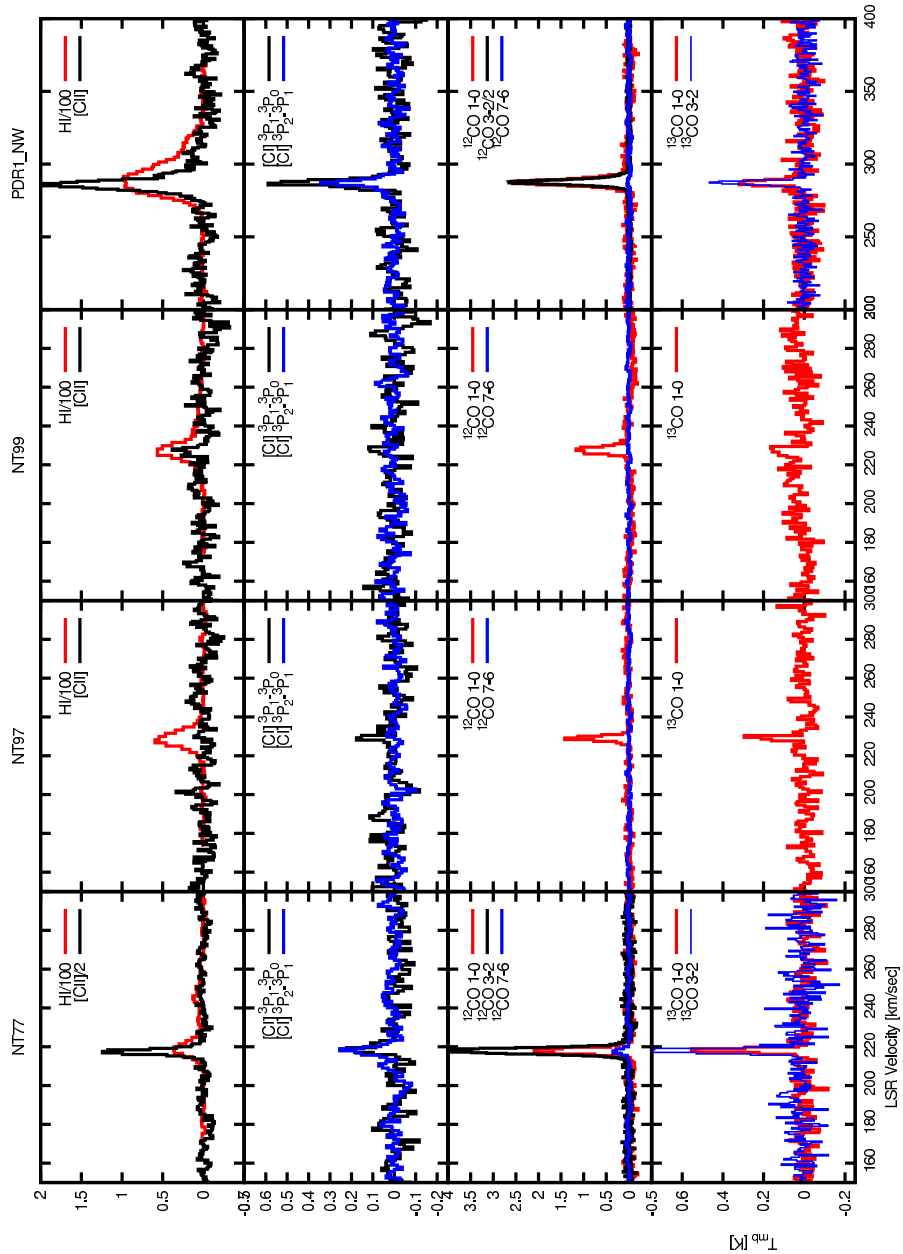


Fig. 10.— (Continued.)

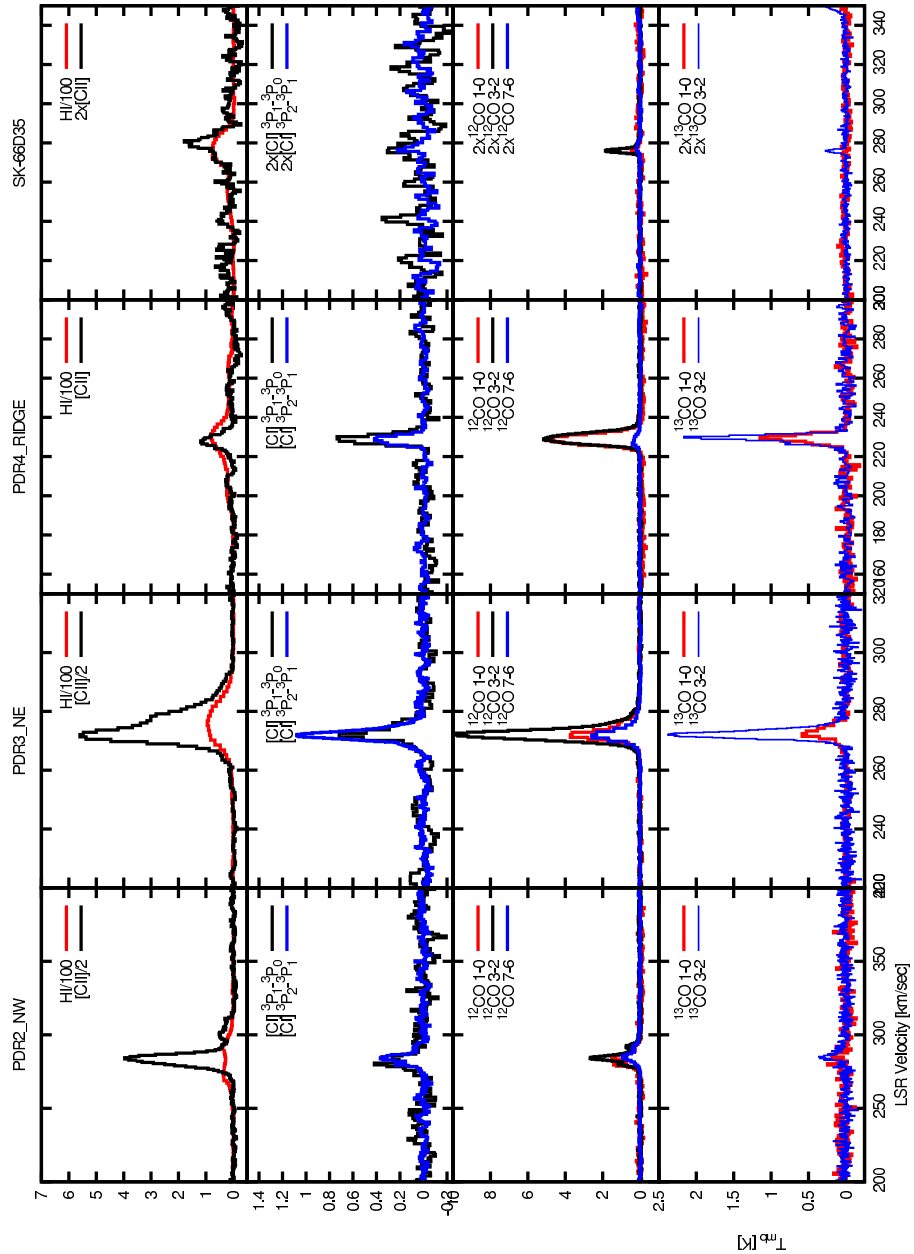


Fig. 11.— (Continued.)

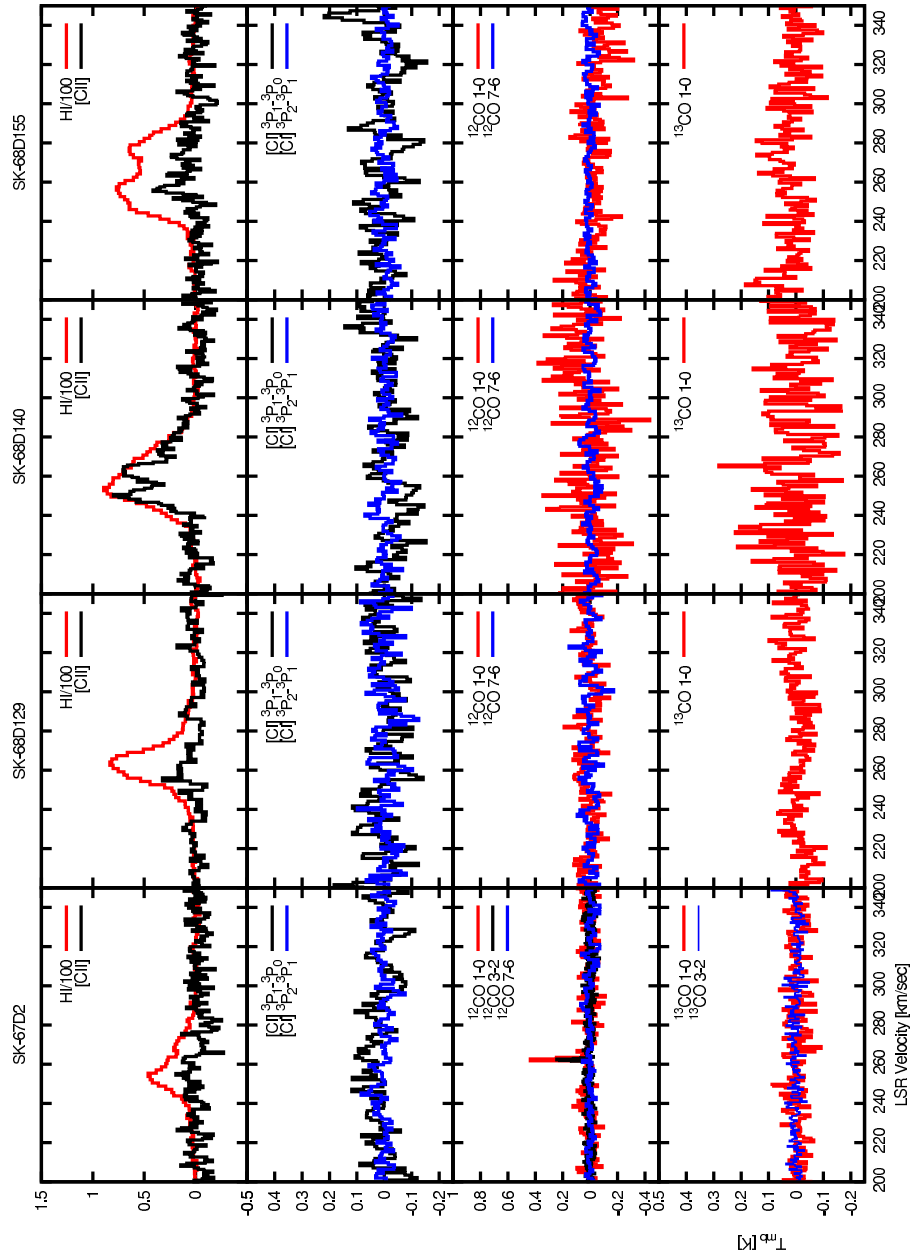


Fig. 12.— (Continued.)

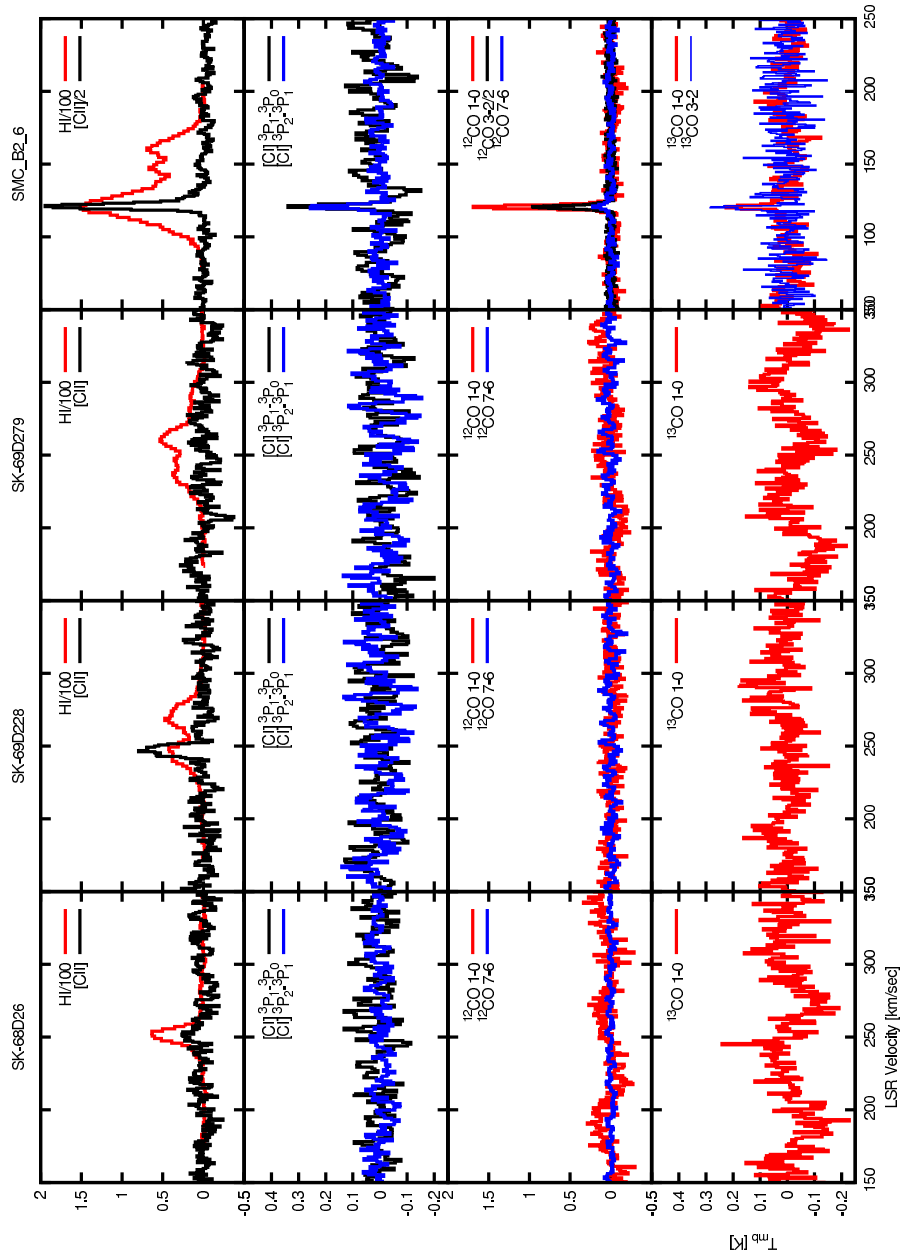


Fig. 13.— (Continued.)

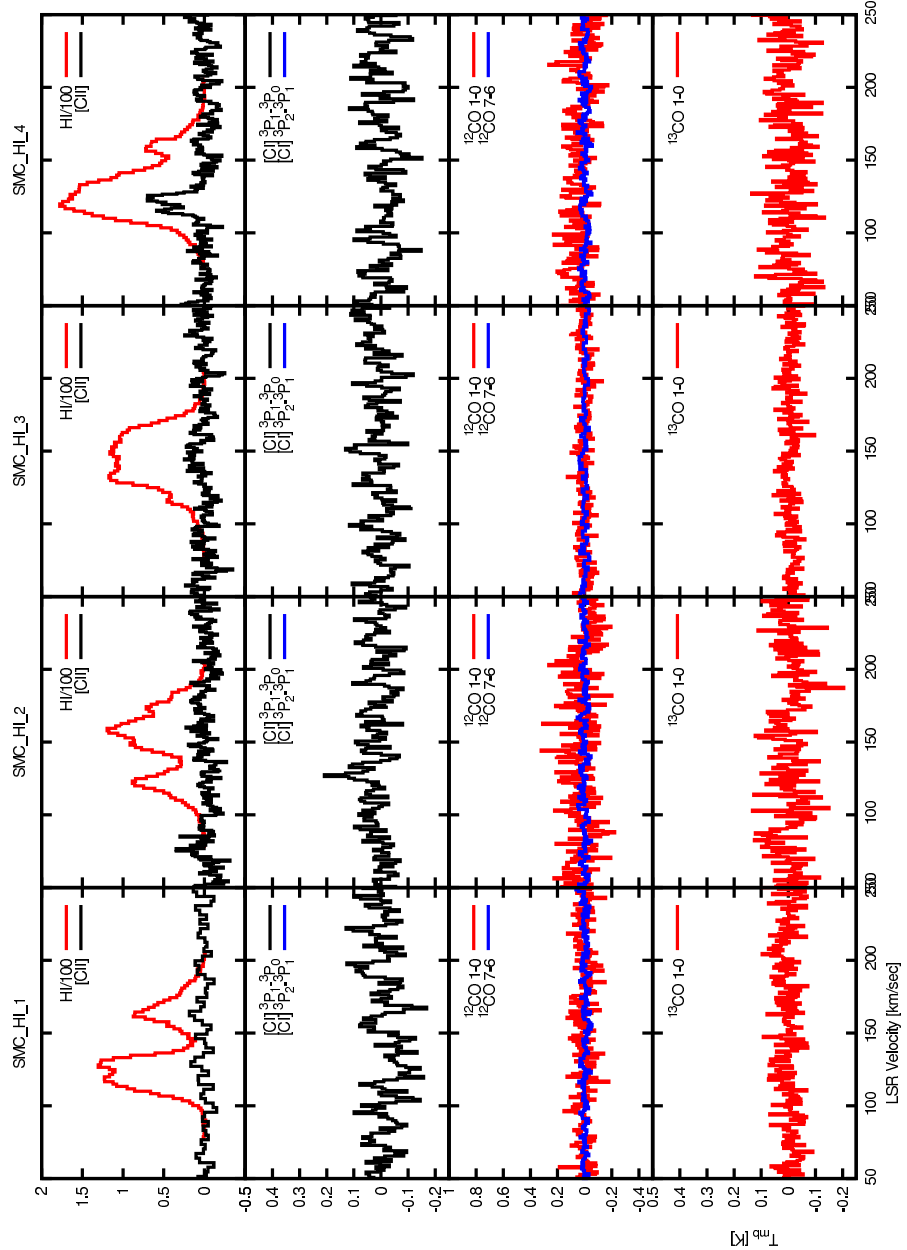


Fig. 14.— (Continued.)

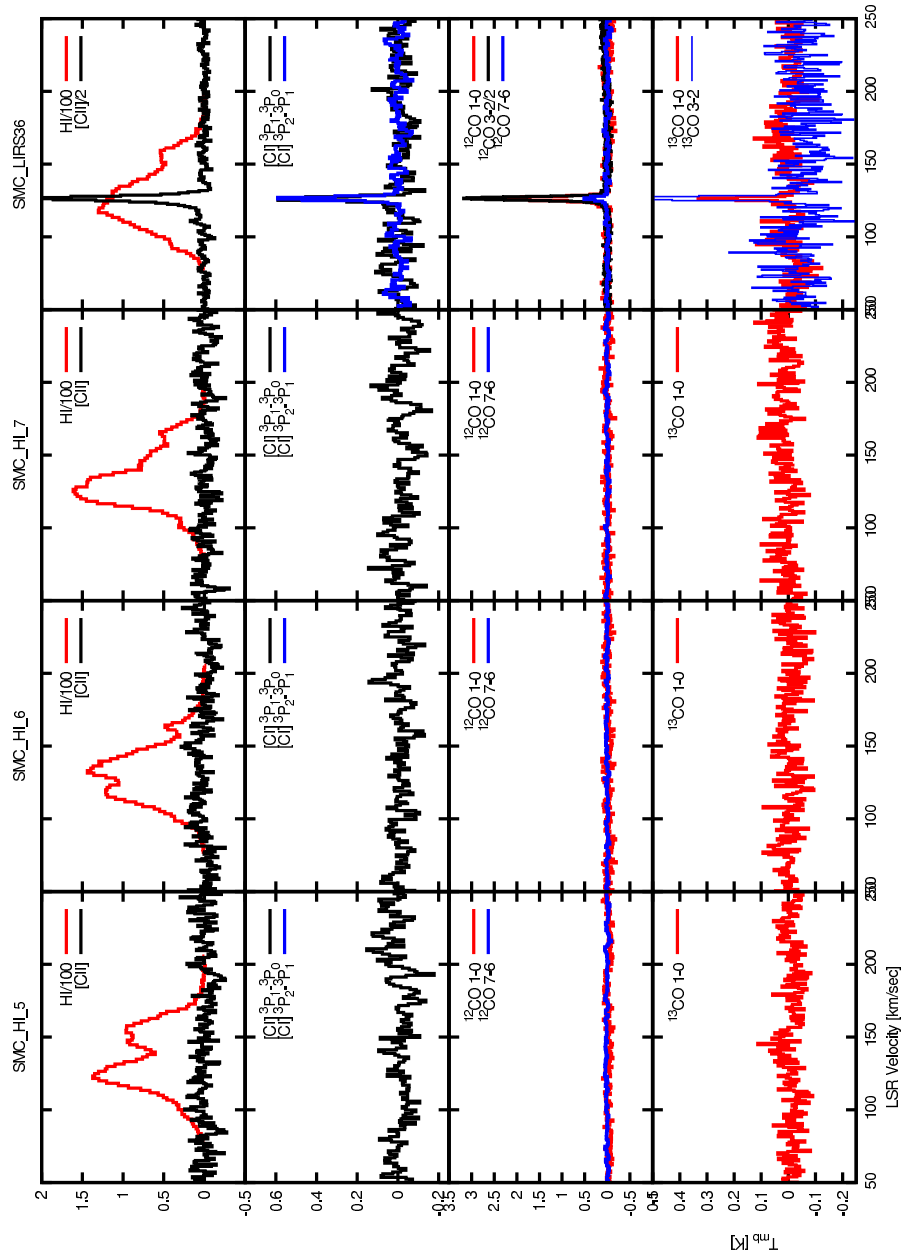


Fig. 15.— (Continued.)

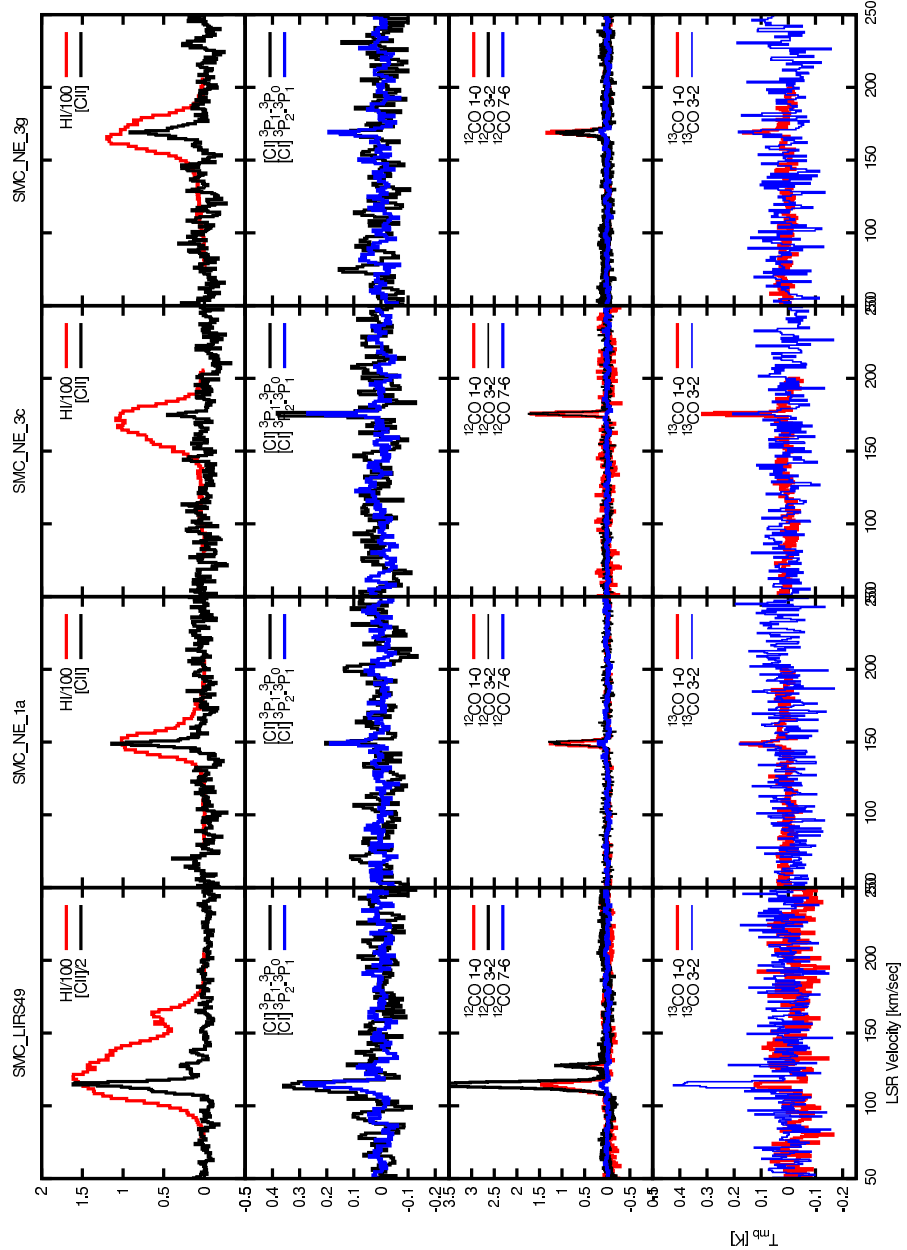


Fig. 16.— (Continued.)

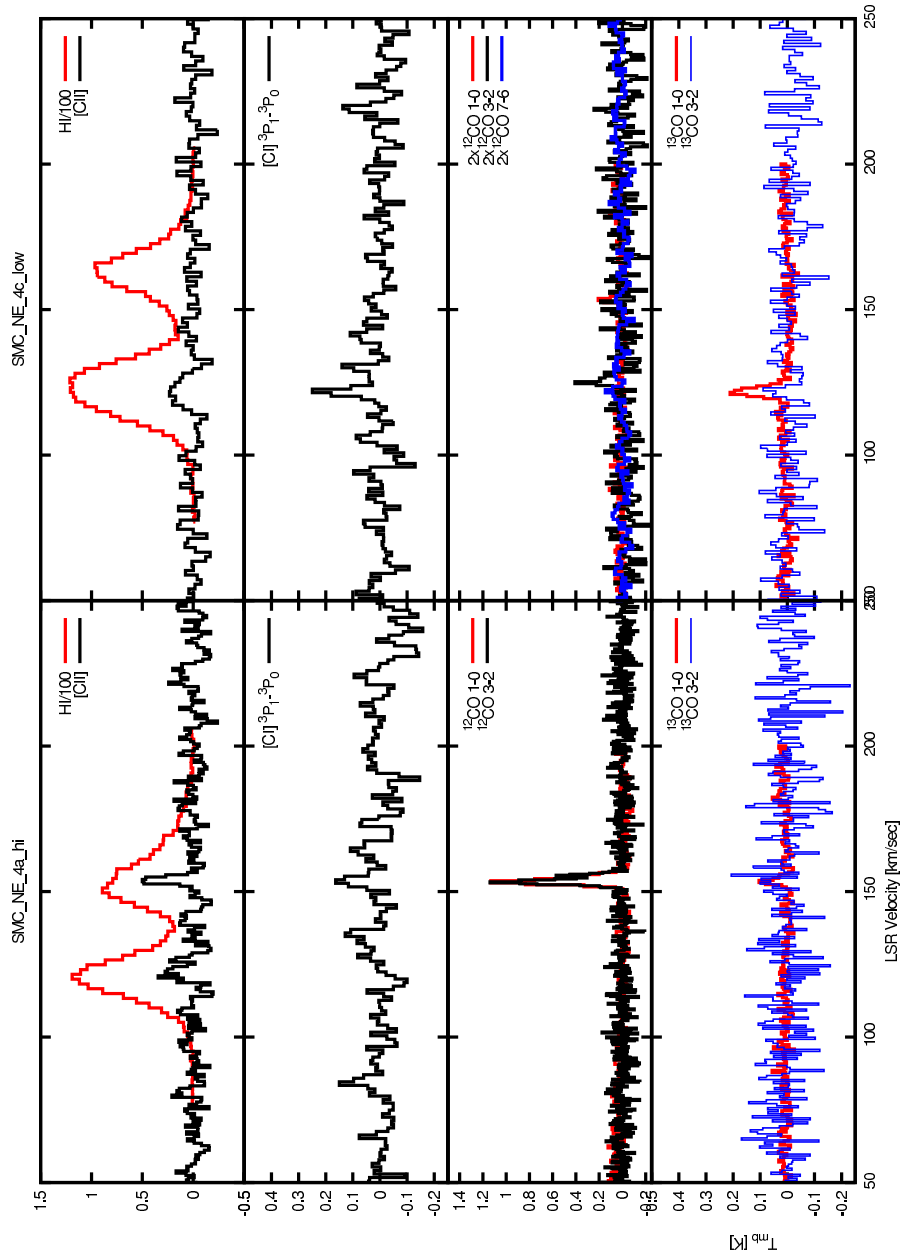


Fig. 17.— (Continued.)